

Insights into the multistep transformation of titanate nanotubes into nanowires and nanoribbons

AGNIESZKA BASZCZUK^{1*}, MAREK JASIORSKI¹, BEATA BORAK¹, JERZY WÓDKA²

¹Wrocław University of Technology, Department of Mechanics, Materials Science and Engineering, Smoluchowskiego 25, 50-370 Wrocław, Poland

²Wrocław University of Technology, Faculty of Chemistry, Smoluchowskiego 23, 50-370 Wrocław, Poland

Different types of titanate one-dimensional nanostructured materials were synthesized and characterized using scanning and transmission electron microscopy, X-ray diffraction and Raman spectroscopy. The results presented in this work unquestionably showed dependence of morphology and structure of the titanate nanopowders on parameters of hydrothermal synthesis. It was found that nanotubes, nanowires and nanoribbons are three unavoidable kinetic products of hydrothermal reaction. Moreover, increasing temperature of reaction or hydrothermal treatment duration results in acceleration of nanotube-nanowire-nanoribbon transformation. However, the sequence of titanate morphology transformation is invariable. The detailed studies further revealed that the crystal structure of hydrothermally prepared nanotubes and nanowires are indistinguishable but the determination of the exact structure is practically impossible. Because of higher crystallinity, the structure of nanoribbons can be established. It was shown that it corresponds to the monoclinic layered trititanic acid $H_2Ti_3O_7$ and is isostructural with sodium derivatives $Na_{2-x}H_xTi_3O_7 \cdot nH_2O$ (with x near 2).

Keywords: *titanate nanotubes; nanoribbons; nanowires; hydrothermal synthesis; structure and morphology*

© Wrocław University of Technology.

1. Introduction

Low dimensional nanostructures such as nanotubes, nanowires, nanofibers and nanobelts have attracted much attention in recent years because of their novel and useful physical properties, leading to numerous potential applications in modern technology [1–5].

Besides the use of low dimensional nanomaterials as interconnection and functional components in designing nano-sized electronics [2] they also find application in gas sensors, catalysts, light-emitting diodes, batteries, solar energy conversion, and so on [3]. Following the discovery of nanotube morphology in carbon [4], it has been shown that a wide range of layered materials is able to form nanotubes. Recently, nanotubes based on metal oxides such as SnO_2 , ZnO , TiO_2 attracted special attention because of their size

and dimensionality dependent electrical, optical and mechanical properties [5]. Among low-dimensional nanostructured metal oxides those based on titanium oxide are considered as the most promising nanostructures. These materials are synthesized by various techniques, however the alkaline hydrothermal method is regarded as the most attractive because of its simple procedures and low cost [6]. Nonetheless, the mechanism of nanostructured titanate materials formation and the method providing the control of morphology (specific shape of material, diameter and length, size distribution) are still the subject of intense research efforts [7]. What is more, our literature survey shows that authors describing titanate structures formed through alkaline hydrothermal treatment have used terms nanoribbons, nanowires, nanorods, nanofibers, nanobelts interchangeably [8]. The clarity in the description of different morphologies concerns only nanotubes because they, as the only one nanostructured titanate material have hollow interior channels. Because

*E-mail: agnieszka.baszczuk@pwr.edu.pl

the terms describing the morphological forms of the materials have not been carefully defined and used in the literature some confusion has resulted and distinctively different morphologies, such as nanotubes, nanofibers, and nanorods, have been reported with apparently similar hydrothermal procedures. As an example it was reported by Yuan *et al.* [9] that the formation of nanotubes and nanoribbons is affected only by the treatment temperature and formation of nanotubes occurs at a temperature range between 100 °C and 180 °C, whereas nanoribbons are formed only at temperatures higher than 180 °C. Similarly, Morgan *et al.* [10] observed phase transition between nanotubes to nanoribbons above 180 °C. However, their analyses of the morphological phase diagram indicated that the effect of temperature was not exclusive in nanoribbon formation and NaOH concentration was a significant contributor. Complete conversion to nanoribbons was observed only in the 10 mol·dm⁻³ NaOH sample treated at 180 °C, whereas lower NaOH concentrations exhibited coexistence of both phases. Morgan *et al.* in their morphological phase diagram showed complex relationship between NaOH concentration, temperature treatment and nanostructure formation and revealed only three different types of morphology: nanoparticles, nanotubes and nanoribbons. In contrast, Lan *et al.* [11] observed at 180 °C the transformation of nanotubes into isolated straight nanorods several micrometers in length and ~400±120 nm in diameter. However, Wu *et al.* [12] showed that high-purity nanotubes are produced even after 30 h of synthesis at 180 °C and transformation to nanowires can be performed after 40 h at 180 °C.

However, it is even more important, that beyond problems with clarity in the description of different morphologies of titanates, our understanding of their crystal structure is incomplete as well. Such information is crucial for prospective applications of titania nanomaterials. It is thus important to reveal the effect of synthesis conditions on the morphology and crystal structure of the hydrothermal products and to introduce standardized description for their different morphological forms. In this report we present detailed transmission

electron microscopy studies together with X-ray diffraction analyses and Raman scattering study on the morphology and crystal structure of products from hydrothermal treatment.

2. Experimental

2.1. Sol-gel synthesis of TiO₂ and hydrothermal synthesis of titanates

The precursor used for one-dimensional titanate nanostructures production was self-prepared TiO₂ powder, which was synthesized by sol-gel method. Titanium isopropoxide, isopropanol, deionized water and aqueous ammonia were used as starting materials in the sol-gel synthesis. Their volume ratio was 3:42:7:4 respectively. The prepared solution was stirred in a plastic flask with a magnetic stirrer at room temperature in contact with atmospheric oxygen for 2 h. Then the titania colloids were allowed to dry yielding finally white powder. At the end, the samples were calcined in air for 2 h at 600 °C.

9 g of TiO₂ prepared this way was put into a Teflon-lined stainless steel autoclave. The autoclave was filled with 500 cm³ 10 M NaOH, maintained at 120 °C, 150 °C or 200 °C for different treatment duration ranging from 10 h to 120 h under vigorous stirring. The final white product was filtered, washed with deionized water and with 1 M HCl at room temperature until the washing solution achieved pH 7. The resulted product was dried in air at 60 °C for 1 h.

2.2. Characterization of TiO₂ powder and titania nanostructures

The surface morphology of the samples was characterized by a scanning electron microscopy (HITACHI S-3400 N) equipped with SE, BSE detectors and EDS system for elemental analysis. Thin carbon layers were deposited (to remove charges) on the surface of the samples before measurements. For more detailed morphological overview of the products high-resolution transmission electron microscopy (FEI Tecnai G² 20 X-TWIN) was used. To determine the phase composition and crystal structure of the materials, X-ray diffraction (XRD) measurement was

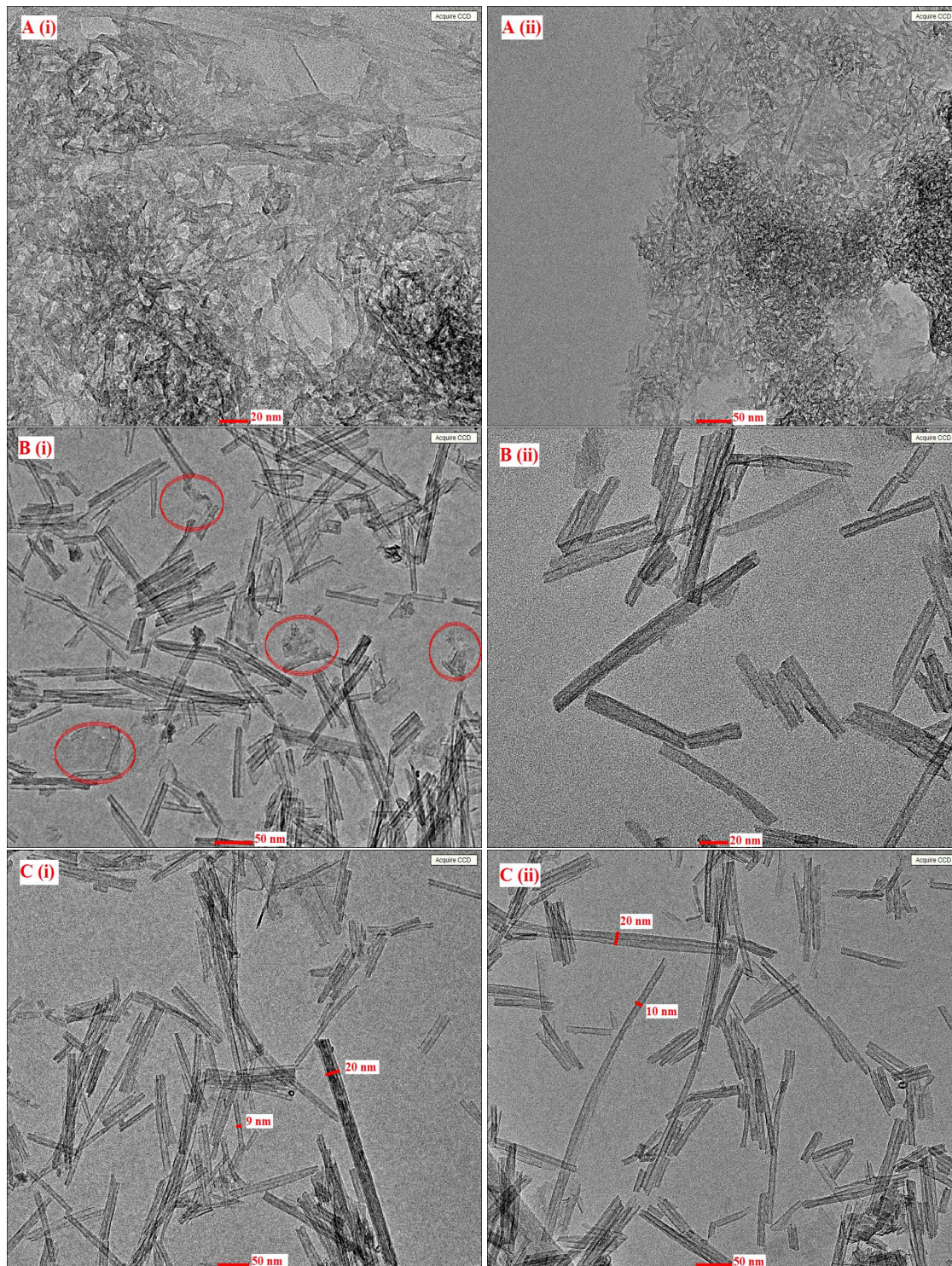


Fig. 1. TEM images of hydrothermal products synthesized at 120 °C for: (A) 24 h, (B) 72 h and (C) 120 h.

carried out at room temperature using a ULTIMA IV/Rigaku/2008 (CuK α with $\lambda = 1.54187 \text{ \AA}$). Raman spectra were measured with Raman system LabRAM HR800, HORIBA JOBIN YVON, 2007.

SEM, XRD and Raman measurements were made in Sol-Gel and Nanotechnology Materials Laboratory of Lower Silesian Center for Advanced Technologies in Wroclaw University of Technology.

3. Results and discussion

We studied the effect of the hydrothermal treatment temperature and duration period on crystal structure and morphology of the products. Fig. 1 to Fig. 3 show a series of SEM and TEM images of the samples synthesized by hydrothermal treatment at different temperatures (120 °C, 150 °C and 200 °C) and different duration time (10 h, 24 h, 72 h and 120 h) followed by washing with 1M HCl. EDX analysis of all samples revealed that there are only trace amounts of sodium left in the materials. So, it can be concluded that the exchange of Na⁺ by H⁺ was complete or, at least, the remaining Na⁺ concentration was below the detection.

It is visible that nanotubes were obtained after 72 h and 120 h at 120 °C (Fig. 1B and Fig. 1C) and 24 h at 150 °C (Fig. 2A), while definitely different nanostructures were formed when other synthesis parameters were used. In addition, after 24 h of hydrothermal treatment at 120 °C, a large amount of lamellar nanosheets were observed (Fig. 1A). Such lamellar structures were reported in literature concerning formation of titanate nanotubes [12, 13] and it was shown that they are unstable due to numerous dangling bonds at the edges, and subsequently wrap and roll up to form nanotubes [13]. Indeed, longer hydrothermal treatment at 120 °C results in transformation of initial lamellar structures into large amount of nanotubes (Fig. 1B) with diameters of about 9 nm and lengths up to 150 nm. Little traces of lamellar nanosheets are still visible what points to the fact that wrapping process is relatively slow. Additionally, Fig. 1B(ii) shows that some of the nanotubes are broken and their fragments aggregate in an oriented way. Further extension of synthesis at 120 °C up to 120 h

leads to elongation of tube length up to several hundreds of nanometers in spite of still observed short fragments of nanotubes (Fig. 1C(ii)). Simultaneously, transformation of nanotubes into non-hollow structures is visible. Such elongation of nanotubes with prolonged reaction time was observed by Lu *et al.* [13] and the process of elongation was described by mixed oriented attachment (OA) and Ostwald ripening mechanism (OR). We observed that long nanotubes self-assemble into bunches what is a clear evidence for an OA mechanism and then bunches of nanotubes gradually transform into nonhollow structures what is typical of OR mechanism. It is widely accepted that solid nanostructures are generally favored over hollow nanotubes in systems after prolonged reaction time but very often such structures are called nanowires, nanorods as well as nanoribbons. Classification giving guidelines to differentiate similar nanostructures was simultaneously suggested by Bavykin *et al.* [8] and Morgan *et al.* [14]. In both papers, the authors carefully described differences between these structures. They described nanowires and nanorods as the same objects differing only in lengths and having low crystallinity. Unlike the nanowires, nanoribbons are described as much longer structures with very good crystallinity and well defined edges. So, according to proposed nomenclature we have classified material produced after the extension of hydrothermal synthesis at 120 °C up to 120 h (Fig. 1C) as nanowires.

It is clear that similar transformation of nanotubes into nonhollow structures is induced by prolonged reaction time or by increase of hydrothermal reaction temperature. Careful analysis of the sample synthesized after the 24 h of hydrothermal treatment at 150 °C reveals that besides nanotubes morphologies predominant nonhollow nanowires are visible (Fig. 2A). The nanowires have poorly defined structure and amorphous layer on external edges. Relatively sharp interfaces are visible along the length of nanowires (Fig. 2A(ii)). Additionally, Fig. 2A(i) shows that some of the nanotubes are broken and some of them have partially filled interior channels what is a clear evidence for the Ostwald ripening mechanism.

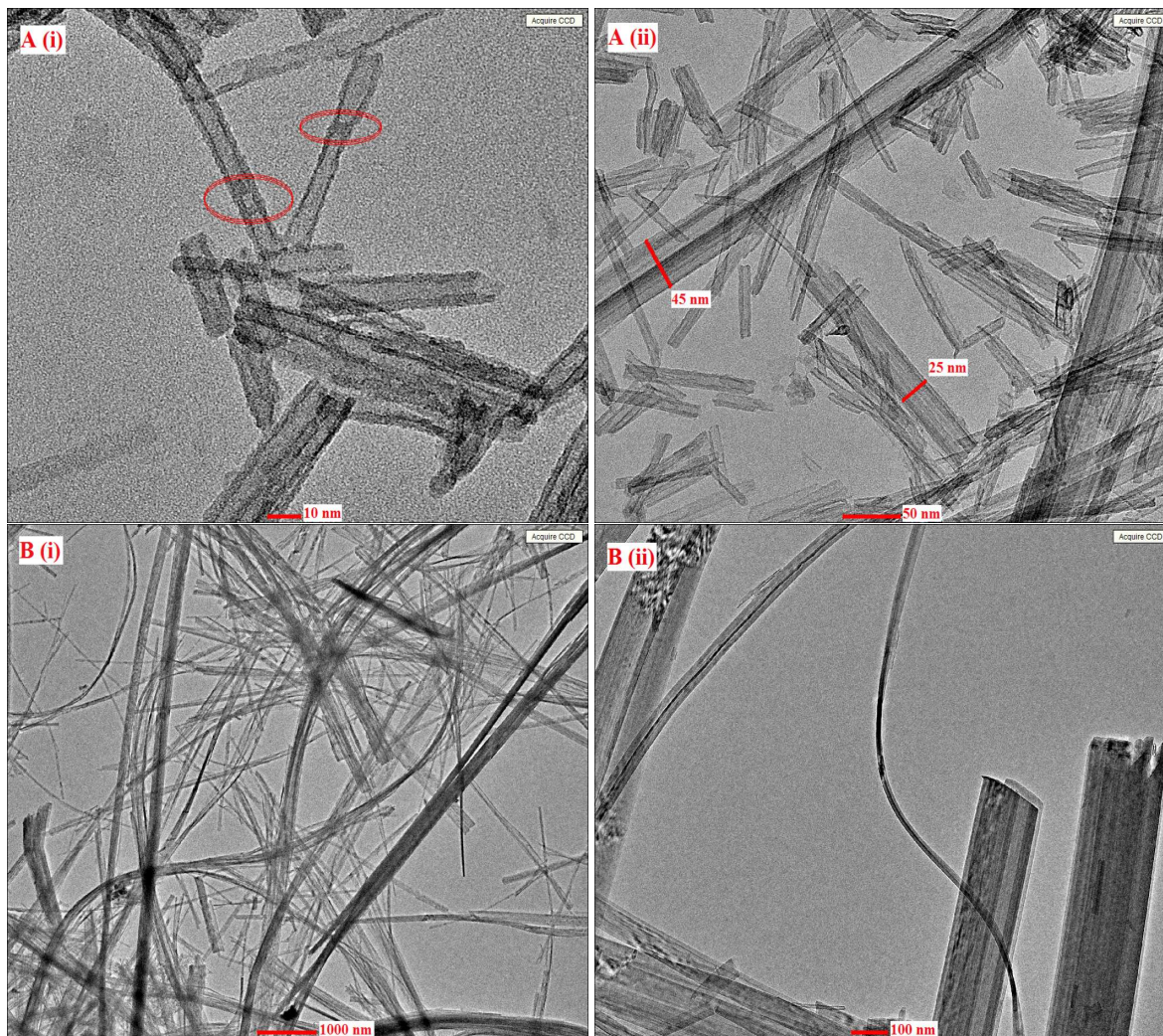


Fig. 2. TEM images of hydrothermal products synthesized at 150 °C for: (A) 24 h and (B) 48 h.

By increasing the treatment duration at 150 °C from 24 h to 48 h nanowires and nanotubes (Fig. 2A) are transformed into much longer and wider elongated structures with well-defined edges and good crystallinity (Fig. 2B). According to further described classification such structures should be defined as nanoribbons. The increase in hydrothermal temperature up to 200 °C results in formation of the same nanoribbons morphology (Fig. 3A and Fig. 3B). So, we observed that actually shorter and having smaller widths nanowires are an intermediate stage before the formation of longer and having larger widths nanoribbons. These results demonstrate that the low crystalline nanotubes are the precursor morphology that

generates, after increasing hydrothermal reaction temperature or/and increasing reaction time, short crystalline nanowires. Subsequently, the nanowires are transformed into final, longer high crystalline nanoribbons. The proposed transformation mechanism between nanotubes and nanowires should be based on co-effects of OR and OA mechanisms while transformation between nanowires and nanoribbons should be explained simply by the improvement of crystallinity.

In order to get a better understanding of the formation mechanism and differences between nanowires and nanoribbons the changes in the crystal structure from the starting raw TiO₂ powder to

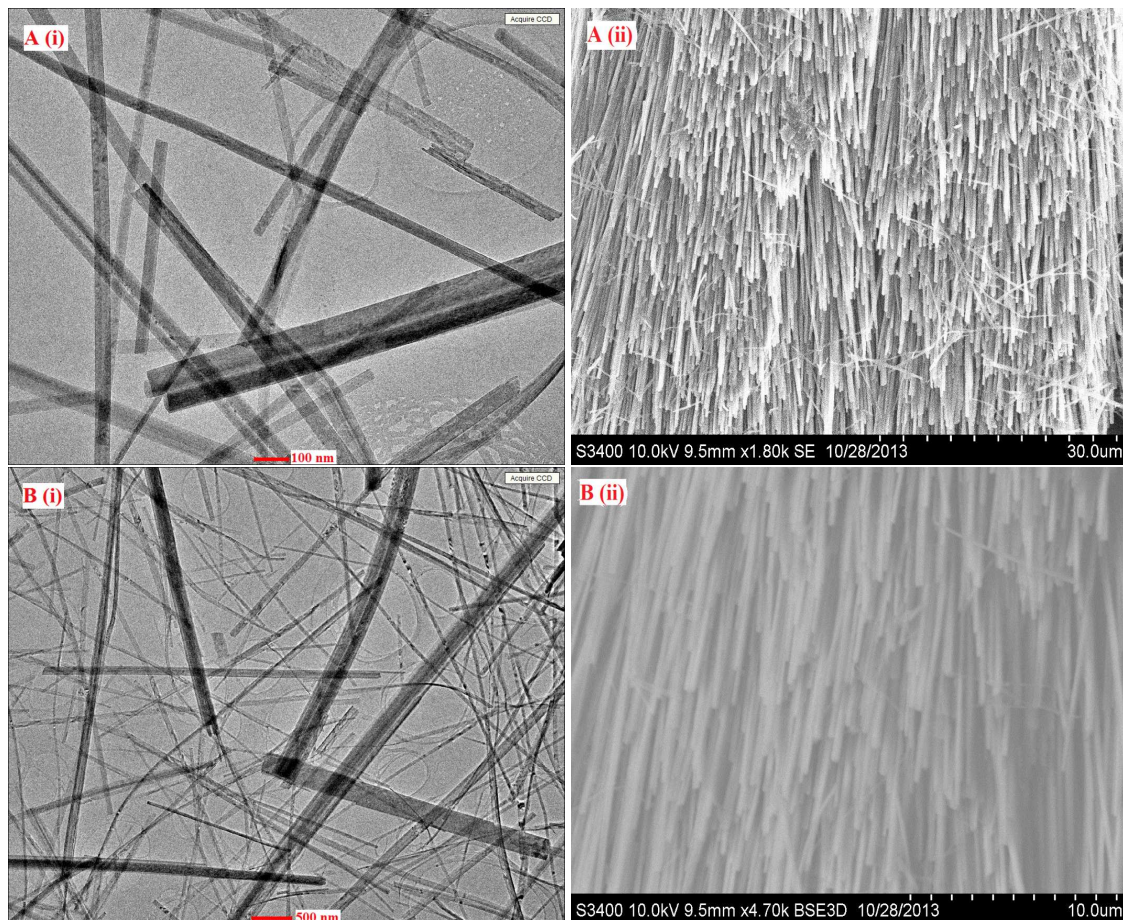


Fig. 3. Electron microscopy images (TEM and SEM) of hydrothermal products synthesized at 200 °C for: (A) 10 h and (B) 24 h.

the samples produced at various hydrothermal reaction times and temperatures were monitored by powder X-ray diffraction (Fig. 4, Fig. 6, Fig. 8). The XRD patterns of materials obtained after hydrothermal synthesis in 120 °C together with that registered for TiO₂ powder used as precursor are presented in Fig. 4.

Analyzing diffraction patterns for samples synthesized at $t = 24$ h and $t = 72$ h it is easy to see that the process of TiO₂ powder precursor transformation into the nanotubular titanates was incomplete what is consistent with TEM observations. Peaks related to anatase and rutile TiO₂ phases are clearly visible for both samples. However, the ratio of the intensity of the strongest anatase reflection to the intensity of the strongest rutile reflection is

changing. As can be seen, by increasing the duration of the hydrothermal treatment the peaks related with anatase become less intensive. These indicates that both anatase and rutile convert into nanotubes at 120 °C, albeit with rutile they are converting at a slower rate. Such observed slower transformation rate of rutile is consistent with the literature [14]. In diffraction patterns for the samples synthesized at $t = 24$ h and $t = 72$ h, besides rather sharp precursor peaks, much broader new peaks indicating the presence of tubular layered titanates are noticeable. All three patterns of the samples exhibit after synthesis a single very broad peak in a low angle region attributed to the interlayer spacing for layered protonic titanates. By increasing the reaction time the broad diffraction peak is shifted from $\sim 6.5^\circ$ to higher values $\sim 10^\circ$

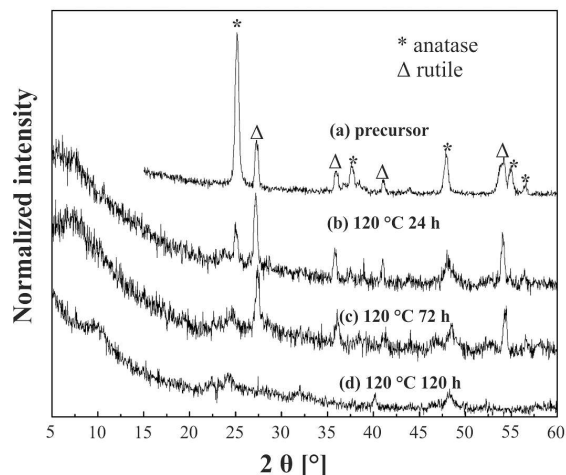


Fig. 4. XRD patterns of materials obtained after hydrothermal synthesis at 120 °C: (b) 24 h, (c) 72 h, (d) 120 h. The XRD pattern of TiO_2 raw powder is given in (a) as reference.

which indicates a decrease of the interlayer spacing (from 14 Å to 9 Å, respectively). This interlayer spacing decrease can be correlated with the release of structural water or it could also indicate transformation from tube to a different nanostructure morphology [15] and is consistent with TEM observations. From Fig. 4 it is clearly visible that only diffraction pattern of the sample synthesized at $t = 120$ h is free of precursor peaks. So, all reflections observed in Fig. 4d must originate from titanate nanostructures, namely nanotubes and a small amount of nanowires. Analyzing diffraction pattern for the sample synthesized at $t = 120$ h, because of broadening of the reflections resulting from small size of the crystals, it is hard to resolve the exact crystal structure of the nanowires. It is widely known that the precise understanding of crystal structure of titanate is incomplete due to some irresolvable problems including large number of crystal modifications for protonated forms of polytitanic acids [8] and simultaneous broadening of the reflections in the XRD pattern. Nowadays, most people agree that the nanotubes made through hydrothermal reaction are layered titanate nanotubes. Our XRD results cannot unambiguously confirm the crystal structure of the synthesized material but are consistent with the

formation of complex layered titanates, in agreement with literature [8, 15]. In order to determine the exact crystal structure of titanate nanotubes several traditional experimental techniques such as electron and X-ray diffraction experiments were used. Due to confusing, sometimes contradictory results a few qualitative structure models were proposed [13, 16]. However, none of the models has been completely tested or refined using Rietveld method because the XRD patterns of nanosized materials show both Bragg-like peaks and a diffuse component. Moreover, the peaks are not as sharp as those in the XRD patterns of the bulk solids [17]. In this context, unconventional techniques involving high-energy XRD and atomic Pair Distribution Function (PDF) analysis can yield the atomic-scale structure of nanosized materials [17, 18] in detail. It is therefore worth reminding that recently, Gateshki et al. [18] irrespective of Pradhan et al. [17] used such unconventional techniques and showed that the $\text{H}_2\text{Ti}_3\text{O}_7$ -type model is the most appropriate for titanate nanotubes. It should be noted that this monoclinic layered trititanic acid phase and more complex derivatives, such as $\text{H}_2\text{Ti}_3\text{O}_7 \cdot n\text{H}_2\text{O}$ [19], $\text{Na}_{2-x}\text{H}_x\text{Ti}_3\text{O}_7$ and $\text{Na}_{2-x}\text{H}_x\text{Ti}_3\text{O}_7 \cdot n\text{H}_2\text{O}$ [8, 20, 21], were also considered in several studies using traditional experimental techniques such as electron and X-ray diffraction experiments.

Trying to better understand the crystal structure of materials produced after hydrothermal synthesis, vibrational spectroscopic methods such as Raman scattering are regarded as an alternative and a useful supplement to the diffraction approaches. Fig. 5 presents Raman spectra obtained for samples after the hydrothermal treatment at 120 °C. It is clearly visible that Raman spectrum for a sample hydrothermally treated for 24 h (Fig. 5a) is noticeably different from that obtained after longer synthesis time (72 h – Fig. 5b, 120 h – Fig. 5c). Precise analysis of Fig. 5a reveals peaks at 143, 514 and 630 cm^{-1} which can be assigned as the E_g , A_{1g} and E_g modes reported for anatase [22] and peaks at 448, 610 cm^{-1} which are in good agreement with reported for E_g and A_{1g} rutile modes [23].

Apart from anatase and rutile Raman bands, additional low intensity peaks are visible in

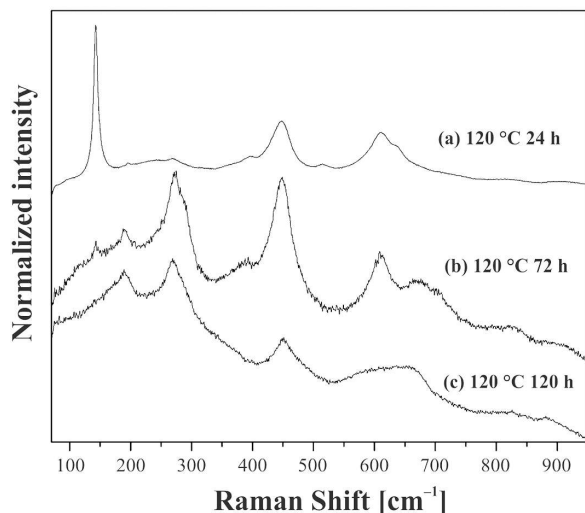


Fig. 5. Raman spectra of materials obtained after hydrothermal synthesis at 120 °C: (a) 24 h, (b) 72 h, (c) 120 h.

the spectrum of the sample treated for shortest time. These peaks are much more intense in the samples hydrothermally treated for 72 h and 120 h. However, one cannot fail to notice that in the spectrum registered for the sample after 72 h, the peaks coming from anatase (142 cm^{-1}) and rutile (609 cm^{-1}) are still present which is consistent with XRD pattern analysis. Both spectra of the samples after prolonged reaction time (72 h and 120 h) exhibit similar broad bands at 190 cm^{-1} , 270 cm^{-1} , 382 cm^{-1} , 448 cm^{-1} , 664 cm^{-1} , $\sim 830\text{ cm}^{-1}$ and $\sim 910\text{ cm}^{-1}$ which are in good agreement with those reported by [24, 25] for orthorhombic titanate ($\text{H}_{0.7}\text{Ti}_{1.825}\text{V}_{0.175}\text{O}_4 \cdot \text{H}_2\text{O}$; V = vacancy). However, their conclusions were based on comparison of the spectra obtained for nanomaterials with that obtained for the well crystallized bulk microcrystalline materials whereas it is well known that size as well as surface induced local distortions of nanomaterials can give rise to substantial changes in the spectroscopic properties in terms of band width and band position [25, 26]. On the other hand, several researchers as for example Gajović *et al.* [27] and Qamar *et al.* [28], after careful *in situ* Raman spectra investigations of different decomposition products, obtained after nanotubes heat treatment postulated monoclinic

$\text{H}_2\text{Ti}_3\text{O}_7$ crystal structure as the most probable. One can note that the bands observed at the spectra measured for our samples (Fig. 5) are also in good agreement with that reported by Gajović and Qamar for $\text{H}_2\text{Ti}_3\text{O}_7$ trititanate and with that described for $\text{Na}_{2-x}\text{H}_x\text{Ti}_3\text{O}_7 \cdot n\text{H}_2\text{O}$ [20, 21] by Ferreira *et al.* It is worth mentioning that according to the authors of the literature [20, 21] the layers of titanium oxides nanotubes are isostructural to the bulk $\text{Na}_2\text{Ti}_3\text{O}_7$ compound.

The influence of the hydrothermal reaction temperature on the samples structure can be seen by comparing the XRD patterns of the material after synthesis at 120 °C and at 150 °C (Fig. 6).

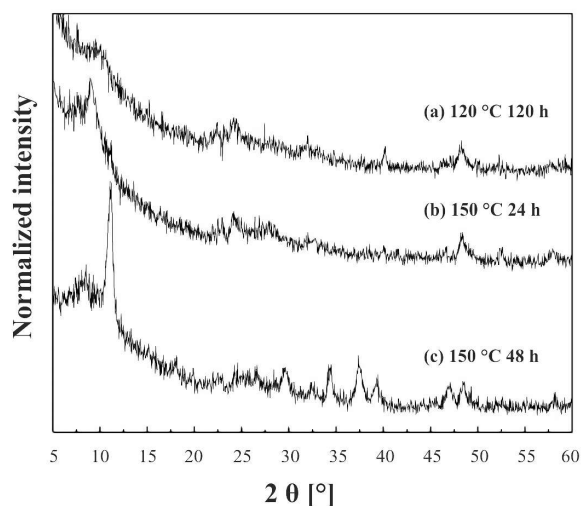


Fig. 6. Comparison between the XRD patterns of the materials synthesized at 120 °C and 150 °C: (a) 120 °C, 120 h, (b) 150 °C, 24 h and (c) 150 °C 48 h.

As revealed by the diffractograms in Fig. 6, by increasing autoclave temperature up to 150 °C it is possible to obtain in 24 hours a material with basically the same morphology and crystal structure as in the synthesis in lower temperature 120 °C in much longer time of 120 hours. From TEM observations it is visible that in both samples nanowires and nanotubes are present, but in different proportions. Samples synthesized at 120 °C for 120 h mostly consist of nanotubes whereas that produced at higher temperature of 150 °C and 24 h are composed mostly of nanowires.

As can be seen from Fig. 6 by increasing the reaction time at temperature fixed at 150 °C the low angle diffraction peak related with the interlayer spacing is narrowing and shifting to higher angles changing from 9.3° to 11.1° as the reaction time varies from 24 h to 48 h. This interlayer spacing decrease can be correlated with the morphology transformation from tube to a distinct shape of material or with the release of structural water. From TEM observations it is clear that nanowires mixed with some nanotubes synthesized at 150 °C for 24 h after the prolongation of synthesis to 48 h convert to nanoribbons. Observed on the TEM images well defined edges and uniform geometry of nanostructures are consistent with a high crystallinity of the sample resulting in sharpness of XRD reflections.

In Fig. 7, Raman spectra measured for samples after the hydrothermal treatment at 150 °C (Fig. 7b and Fig. 7c) are presented. For comparison purposes the spectrum for the sample hydrothermally treated at 120 °C for 120 h is also presented (Fig. 7a). It is visible that the spectra measured for the samples treated at 120 °C for 120 h and 150 °C for 24 h are almost identical reflecting bands reported by Gajović et al. [27] and Qamar et al. [28] for $\text{H}_2\text{Ti}_3\text{O}_7$ trititanate. Bearing in mind observations provided by TEM and XRD experiments, it can be concluded that both nanotubes and nanowires may have the same crystal structure. Such conclusion is also in line with results presented by Ferreira et al. [20, 21] for hydrothermally produced $\text{Na}_{2-x}\text{H}_x\text{Ti}_3\text{O}_7 \cdot n\text{H}_2\text{O}$ nanomaterials. Raman spectrum for the sample hydrothermally treated at 150 °C for a longer time (48 h) is noticeably different from the spectrum obtained after 24 h. After prolonged synthesis, Raman bands split into several components and become narrower what seems to be caused by the increase of crystallinity. Some authors associate such Raman spectrum change with the crystal structure transformation but there is no clear evidence of this. As it was discussed earlier, the broadening of the reflections in the XRD pattern or Raman bands prevents resolving the exact crystal structure. Broad Raman bands result from low crystallinity or small size

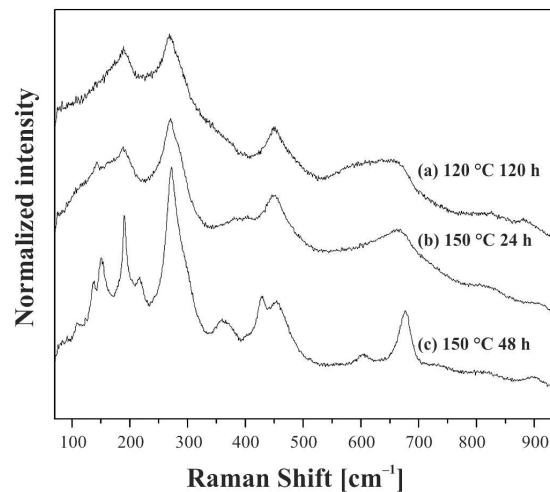


Fig. 7. Raman spectra of materials obtained after hydrothermal synthesis at 150 °C: (b) 24 h, (c) 48 h and as a reference Raman spectrum of material synthesized at 120 °C for 120 h (a).

of crystals [20, 21, 29] and they can contain non-separated reflection components that may be visible after the enhancement of crystallinity.

The change in Raman spectra, namely an increase in the peak numbers and their relative intensity and sharpness between samples with $t = 24$ h and $t = 48$ h can be also supported by the observed in TEM images transformation from nanotubes to much more crystalline nanoribbons morphology. The spectrum for sample hydrothermally treated at 150 °C for 48 h is basically similar to that obtained by Kolen'ko et al. [30] and Papp and co-workers [31] for $\text{H}_2\text{Ti}_3\text{O}_7$. It also corresponds to the Raman spectrum presented for $\text{Na}_{2-x}\text{H}_x\text{Ti}_3\text{O}_7 \cdot n\text{H}_2\text{O}$ titanates [20, 21].

Fig. 8 presents the XRD patterns of materials obtained after hydrothermal synthesis at 200 °C for 10 h and 24 h together with that registered for the samples treated at 150 °C for 48 h.

Notice that the patterns measured for the samples from the synthesis at 200 °C are very similar to those registered for the samples treated at 150 °C for 48 h what perfectly correlates with very similar shapes of nanostructures, namely nanoribbons observed in TEM images. As can be seen, after the enhancement of crystallinity by

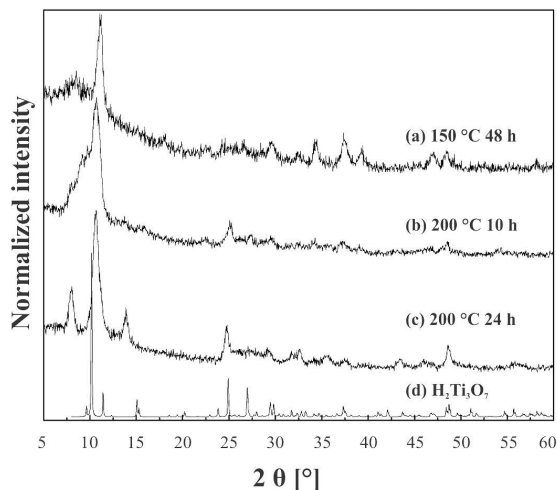


Fig. 8. XRD patterns of materials after hydrothermal synthesis at 200 °C: (b) 10 h, (c) 24 h and material after hydrothermal synthesis at 150 °C for 72 h (a). The XRD pattern of $\text{H}_2\text{Ti}_3\text{O}_7$ generated using the data deposited in ICSD database by Gateshki *et. al.* [18] is given in (d) as reference.

increasing the duration of the hydrothermal treatment at 200 °C from 10 h to 24 h, the XRD peaks become narrower and new peaks are detected. So, the phase analysis of such well crystalline material was finally possible. We generated the XRD pattern of $\text{H}_2\text{Ti}_3\text{O}_7$ using the data deposited in ICSD database by Gateshki *et al.* [18] and noticed that the diffraction peaks of all samples shown in Fig. 8 can be assigned to the reflections of the monoclinic trititanate. The type of crystal structure proposed for nanoribbons is based on the $\text{H}_2\text{Ti}_3\text{O}_7$ model put forward by Gateshki *et al.* [18] for nanotubes obtained after an atomic pair distribution function (PDF) analysis, which is known to be well-suited for materials with limited structural coherence. The $\text{H}_2\text{Ti}_3\text{O}_7$ -type model was used by them for the description of nanotubes crystal structure, however we have noticed that it perfectly fits to the nanoribbons. Bearing in mind the observations provided by TEM and XRD experiments, it can be concluded that nanotubes, nanowires and nanoribbons may have the same crystal structure. It is worth mentioning that isostructural crystal structures of nanotubes and nanoribbons were also proposed on the basis of the Raman spectroscopy in [20, 21] for more complex sodium derivatives of $\text{H}_2\text{Ti}_3\text{O}_7$.

In Fig. 9, Raman spectra measured for the samples after the hydrothermal treatment at 200 °C for 10 h (Fig. 9b) and 24 h (Fig. 9c) are presented.

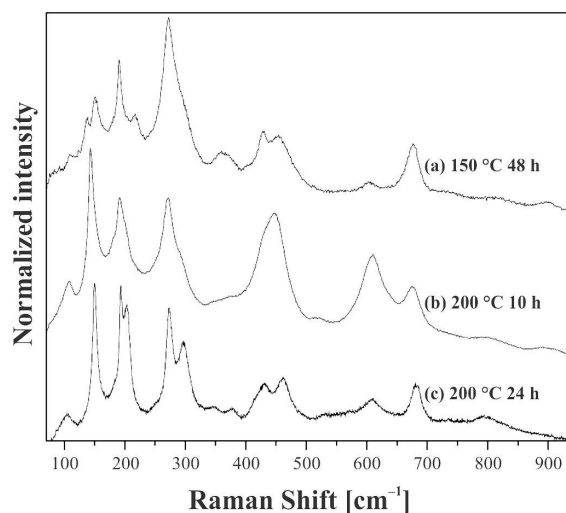


Fig. 9. Raman spectra of materials obtained after hydrothermal synthesis at 200 °C: (b) for 24 h, (c) for 10 h and as a reference Raman spectrum of material synthesized at 150 °C for 48 h (a).

The spectrum for the sample hydrothermally treated at 150 °C for 48 h is also presented as a reference. Notice that the spectra measured for the samples from the synthesis at 200 °C are very similar to those of registered for samples treated at 150 °C for 48 h just as in case of XRD patterns. Such similarity perfectly correlates with very similar shape of nanostructures, namely the nanoribbons observed in TEM images.

4. Conclusions and final remarks

The influence of the hydrothermal reaction temperature on the synthesized nanomaterial properties was evaluated by studying samples prepared at 120 °C, 150 °C, 200 °C for different autoclave dwell time. The best experimental conditions to prepare the titanate nanotubes structures were set at 120 °C and 72 h and at 150 °C and 24 h. Definitely, different nanostructures were formed when other synthesis parameters were used. Nanotubes produced at the lowest temperature of 120 °C were accompanied with precursor powder when the synthesis time was insufficient or with nanowires

when the time of synthesis was prolonged. Similar transformation of nanotubes into nanowires was observed after 24 h at 150 °C. By increasing the treatment duration at 150 °C from 24 h to 48 h nanowires and nanotubes had transformed into much longer and wider elongated structures with well-defined edges and good crystallinity, called nanoribbons. The observed temperature of nanotubes to nanoribbons transformation (150 °C) was much lower than the recommended in the literature 180 °C [9, 10] but was enhanced by the prolonged synthesis time. The same types of nanostructures, namely nanoribbons were observed when the hydrothermal reaction temperature increased to 200 °C.

We showed that although authors describing titanate structures formed through alkaline hydrothermal treatment used the terms nanoribbons and nanowires interchangeably, these types of structures are different. Even though the nanotubes can be transformed into both the nanowires and nanoribbons the parameters needed for the transformation process are completely different. Nanowires, which are typical of lower hydrothermal synthesis temperatures and shorter reaction times have the aspect ratio (length divided by diameter) as close as possible to the nanotubes while nanoribbons with the values typically between several dozen nm and several hundred nm are much longer. More importantly, the level of crystallinity is really low for both nanowires and nanotubes. The nanoribbons which are typical of higher hydrothermal synthesis temperatures have well defined edges, rather uniform geometry and tend to have high crystallinity. We showed that the crystal structures of hydrothermally prepared nanotubes and nanowires are indistinguishable and the determination of the exact structure is practically impossible. The crystal structure of nanoribbons because of their higher crystallinity can be established and it corresponds to the monoclinic layered trititanic acid $\text{H}_2\text{Ti}_3\text{O}_7$ and its isostructural sodium derivatives $\text{Na}_{2-x}\text{H}_x\text{Ti}_3\text{O}_7 \cdot n\text{H}_2\text{O}$ (with x close to 2). Based on Raman spectra investigation and analysis of available literature data we assume that nanoribbons, nanowires and nanotubes may have the same

crystal structure and they differ only in the degree of crystallinity. Nanotubes, nanowires and nanoribbons are three unavoidable kinetic products of hydrothermal reaction. By increasing temperature of reaction or annealing time the nanotube-nanowire-nanoribbon transformation process is accelerated but the sequence of titania morphology is invariable.

Acknowledgements

The research was supported by the Wrocław Research Centre EIT+ within the project “The Application of Nanotechnology in Advanced Materials” – NanoMat (POIG.01.01.02-002/08), co-financed from the resources of the European Regional Development Fund (POIG 1.1.2) and by the Department of Mechanics, Materials Science and Engineering, Wrocław University of Technology under Contract No. S50105/K1010.

References

- [1] TIWARI J.N., TIWARI R.N., KIM K.S., *Prog. Mater. Sci.*, 57 (2012), 724.
- [2] FANG X., ZHANG L., *J. Mater. Sci. Technol.*, 22 (2006), 1.
- [3] XIA Y., YANG P., SUN Y., WU Y., MAYERS B., GATES B., YIN Y., KIM F., YAN H., *Adv. Mater.*, 15 (5) (2003), 353.
- [4] IIJIMA S., *Nature*, 354 (1991), 56.
- [5] RAMASAMY P., LIM D.-H., KIM J., KIM J., *RSC Adv.*, 4 (2014), 2858.
- [6] TOHR S., *Inorganic and Metallic Nanotubular Materials*, Springer, Berlin Heidelberg, 2010, p. 17.
- [7] BAVYKIN D.V., WALSH F.C., *Eur. J. Inorg. Chem.*, 8 (2009), 977.
- [8] BAVYKIN D.V., FRIEDRICH J.M., WALSH F.C., *Adv. Mater.*, 18 (2006), 2807.
- [9] YUAN Z.-Y., SU B.-L., *Colloid. Surface. A*, 241 (2004), 173.
- [10] MORGAN D.L., ZHU H.-Y., FROST R.L., WACLAWIK E.R., *Chem. Mater.*, 20 (2008), 3800.
- [11] LAN Y., GAO X., ZHU H., ZHENG Z., YAN T., WU F., RINGER S.P., SONG D., *Adv. Funct. Mater.*, 15 (2005), 1310.
- [12] WU D., LIU J., ZHAO X., LI A., CHEN Y., MING N., *Chem. Mater.*, 18 (2006), 547.
- [13] LU H., ZHAO J., LI L., ZHENG J., ZHANG L., GONG L., WANG Z., ZHU Z., *Chem. Phys. Lett.*, 508 (2011), 258.
- [14] MORGAN D.L., TRIANI G., BLACKFORD M.G., RAFTERY N.A., FROST R.L., WACLAWIK E.R., *J. Mater. Sci.*, 46 (2011), 548.
- [15] YLHÄINEN E.K., NUNES M.R., SILVESTRE A.J., MONTEIRO O.C., *J. Mater. Sci.*, 47 (2012), 4305.
- [16] MA R., BANDO Y., SASAKI T., *Chem. Phys. Lett.*, 380 (2003), 577.

- [17] PRADHAN S.K., MAO Y., WONG S.S., CHUPAS P., PETKOV V., *Chem. Mater.*, 19 (2007), 6180.
- [18] GATESHKI M., CHEN Q., PENG L.-M., CHUPAS P., PETKOV V., *Z. Kristallogr.*, 222 (2007), 612.
- [19] SUZUKI Y., YOSHIKAWA S., *J. Mater. Res.*, 19 (2004), 982.
- [20] FERREIRA O.P., SOUZA FILHO A.G., FILHO J.M., ALVES O.L., *J. Braz. Chem. Soc.*, 17 (2006), 393.
- [21] VIANA B.C., FERREIRA O.P., SOUZA FILHO A.G., FILHO J.M., ALVES O.L., *J. Braz. Chem. Soc.*, 20 (2009), 167.
- [22] ZHANG W.F., HE Y.L., ZHANG M.S., YIN Z., CHEN Q., *J. Phys. D Appl. Phys.*, 33 (2000), 912.
- [23] KRISHNAMURTI D., *P. Indian AS-Sec. A*, 55 (1962), 290.
- [24] GAO T., FJELLVLÍG H., NORBY P., *Inorg. Chem.*, 48 (2009), 1423.
- [25] MA R., FUKUDA K., SASAKI T., OSADA M., BANDO Y., *J. Phys. Chem. B*, 109 (2005), 6210.
- [26] RISS A., BERGER T., STANKIC S., BERNARDI J., KNÖZINGER E., DIWALD O., *Angew. Chem. Int. Edit.*, 47 (2008), 1496.
- [27] GAJOVIĆ A., FRIŠČIĆ I., PLODINEC M., IVEKOVIĆ D., *J. Mol. Struct.*, 924 – 926 (2009), 183.
- [28] QAMAR M., YOON C.R., OH H.J., KIM D.H., JHO J.H., LEE K.S., LEE W.J., LEE H.G., KIM S.J., *Nanotechnology*, 17 (2006), 5922.
- [29] GOUADEC G., COLOMBAN P., *Prog. Cryst. Growth Ch.*, 53 (1) (2007), 1.
- [30] KOLEN'KO Y.V., KOVNIR K.A., GAVRILOV A.I., GARSHEV A.V., FRANTTI J., LEBEDEV O.I., CHURAGULOV B.R., VAN TENDELOO G., YOSHIMURA M., *J. Phys. Chem. B*, 110 (2006), 4030.
- [31] PAPP S., KÖRÖSI L., MEYNEN V., COOL P., VANSANT E.F., DÉKÁNY I., *J. Solid State Chem.*, 178 (2005), 1614.

Received 2015-08-20

Accepted 2016-07-26